

## DETERMINATION OF PHOTOCATALYTIC ACTIVITY FOR THE SYSTEM: CdS CHEMICAL BATH DEPOSITED THIN FILMS COATED WITH TiO<sub>2</sub> NPs

E. PALMA-SOTO<sup>a</sup>, M. DE LA LUZ MOTA-GONZÁLEZ<sup>a,b</sup>,  
P. A. LUQUE-MORALES<sup>c</sup>, AMANDA CARRILLO- CASTILLO<sup>a,\*</sup>

<sup>1</sup>*Institute of Engineering and Technology, Autonomous University of Ciudad Juárez. Cd. Juárez Chihuahua. CP 32310, México*

<sup>2</sup>*CONACYT- Autonomous University of Ciudad Juárez. Cd. Juárez Chihuahua. CP 32310, México*

<sup>3</sup>*Faculty of Engineering, Architecture and Design, Autonomous University of Baja California, Ensenada Baja California. C.P. 22860, México*

At this research, it is proof the degradation of methylene blue colorant, as photocatalytic activity, which result from the interaction between a CdS thin film surface, coated by TiO<sub>2</sub> NPs, and the molecules of an aqueous solution of methylene blue colorant. This heterogeneous device, TiO<sub>2</sub> NPs/CdS thin film/Glass substrate, pump by solar radiation; can be used to wastewater treatment. CdS thin films, are deposited by chemical bath deposition, while the TiO<sub>2</sub> nanoparticles (Nps) were obtained by a microwave-assisted sol-gel process method and deposited on CdS layer by spin coating technique. The main syntheses used techniques for these materials, are parts of the soft chemistry. The optical characterization of, TiO<sub>2</sub> NPs/CdS thin films/Glass substrate, was evaluated by UV-vis spectroscopy, and the calculated band gap for the films was 2.8 eV. Agglomerations of TiO<sub>2</sub> nanoparticles were observed on the homogeneous surface of polycrystalline hexagonal structure of the CdS thin films. The degradation of methylene blue colorant is carry out by three replicates of TiO<sub>2</sub>/NPs/CdS thin films/Glass substrate, exposed to sunlight for 60 minutes, resulting in a degradation of 43%.

(Received November 9, 2020; Accepted February 2, 2021)

*Keywords:* Chemical bath deposition; Cadmium sulphide; TiO<sub>2</sub> NPs, Complexing agent

### 1. Introduction

Nowadays, environmental problems such as increased air and water pollution have expanded due population growth and rapid industrial development worldwide [1]. The methylene blue (MB) is one of the most frequently used compounds to model the organic pollutants found in wastewater discharges in various industries [2], is a highly stable toxic compound and it is a type of thiazine dye very commonly used in industry [3]. Based on this, heterogeneous photocatalysis is used to degrade organic pollutants in wastewater that are discharged into the ecosystem and it has been demonstrated as an effective technology for treating groundwater, drinking water, wastewater, and air pollution [4-5]. When compared to conventional filtration methods, heterogeneous solar photocatalysis observes advantages that include low temperature operation, minimal corrosion of handling equipment [6], no need of chemical additives, and the generation of innocuous or easily neutralized reaction by-products [7]. Solar energy photocatalysis is used to activate semiconductor materials that result in the creation of hydroxyl radicals, which discolor organic pollutants dissolved in water [8].

Titanium dioxide (TiO<sub>2</sub>) is an inorganic semiconductor material type n that absorbs electromagnetic radiation in the ultraviolet region (UV, > 400 nm) [9]. There are several physical and chemical methods for the synthesis of Nano scale TiO<sub>2</sub> materials [10], obtaining a variety of nanostructures such as nanoparticles, nanotubes, Nano rods and nanofibers. For this investigation, the sol-gel method was selected to prepare the TiO<sub>2</sub> in powder. The sol-gel synthesis is simple, inexpensive, and it is a process at low temperature. This method has been used to produce high

---

\* Corresponding author: amanda.carrillo@uacj.mx

purity nanoparticles (NPs) of various catalytic materials (mainly metal oxides) such as  $ZrO_2$ ,  $SrTiO_3$ ,  $ZnO$ ,  $WO_3$ , and  $TiO_2$  [11-12]. The use of  $TiO_2$  as a photocatalytic material has some important benefits that include a low price of feedstock reagents, the ability to synthesize at room temperature, and the generation of innocuous byproducts after synthesis (i.e.,  $CO_2$  and  $H_2O$ ) [13]. From a photocatalytic property perspective,  $TiO_2$  has the peculiarity of showing photochemical stability and high oxidation power in the UV region, high resistance to photo corrosion in aqueous environments, and lower cost when compared to other photocatalytic materials [14]. Nevertheless, the primary disadvantage of using  $TiO_2$  is associated to its exclusive activation in the ultraviolet region, and hence it only takes advantage of around 3-5% of the sunrays that reach the surface of the planet. This limitation has driven the interest in researching other materials that can be coupled with  $TiO_2$  for a greater use of the sunlight spectrum [15].

In this context, cadmium sulfide (CdS) is a photocatalyst that is excited by the photons that fall on the visible spectrum region (from 400 nm to 750 nm) and as is considered a binary semiconductor, it belongs to the II–VI group and has a band gap of 2.4 eV [16- 19]. The CdS has a high photocatalytic activity that allows a better use of the sunlight spectrum i.e., from 40% up to 50%., as opposed to more commonly reported lower thresholds at 4% to 5% [20]. The use of CdS extends the functionality of  $TiO_2$  in the visible region. CdS thin films can be synthesized using the chemical bath deposition (CBD) technique [21].

By separate, CdS and  $TiO_2$  have problems that include reduced efficiency, exhibit photo-corrosion and become unstable to photo-radiation (in the case of CdS) or have a wide band gap that reduces the absorption of solar energy (for  $TiO_2$ ). Nevertheless, the combination of CdS with  $TiO_2$  overcomes these issues [22-24], the junction  $TiO_2$ /CdS, is a new kind of n-n semiconductor, with good absorption in both the UV and visible regions of the spectrum. In combination, CdS and  $TiO_2$  overcome their individual limitations, achieving a high photocatalytic activity [25], and besides extending the response from UV to visible light, this type of semiconductor depresses recombination of the photo excited electrons and holes, has no problems of photo-corrosion, and it is highly stable [26]. Previous works reported the synthesis and photocatalytic activity of CdS/ $TiO_2$  composites synthesized with the use of high temperature or long time of the synthesis: by electrospinning method [27], hydrothermal treatment [28-30], varying of precursor concentration with thermal annealing of the final product [31-32], and by simple soft chemistry assisted by thermal annealing [33- 38].

This work presents the use of low-energy soft chemistry for the preparation of composed CdS thin film surface, coated by  $TiO_2$  NPs, as a photocatalytic material with an expanded spectrum of absorbance in the ultraviolet and visible spectrums, taking advantage up to 55% of the solar radiation [39]. The photocatalytic activity (PC) of the resulting composite material was tested by degrading of MB in an aqueous solution showing the reduction of this contaminant in an aqueous solution model.

## 2. Experimental details

### 2.1. Materials

The preparation of the CdS thin films was carried out using the following reagents from commercial sources: cadmium chloride ( $CdCl_2$ , 99%) (Supplied from Across, US), sodium citrate ( $Na_3C_6H_5O_7$ , 99.8%) (Provided by Fermont, Nuevo León, México), thiourea ( $CH_4N_2S$ , 99.4%) (Provided by J.T. Baker, Edo. De México, México), potassium hydroxide (KOH, 87.3%) (Obtained by Fermont, Nuevo León, México) and borate buffer solution (pH of 10) (Provided by J.T. Baker, Edo. De México, México).

For the preparation of  $TiO_2$  nanoparticles, the following reagents were used: titanium isopropoxide ( $C_{12}H_{28}O_4Ti$  97%) (Provided by Sigma-Aldrich, Toluca, México), 2-propanol ( $C_3H_8O$  99.8%) (Provided by Fermont, Nuevo León, México) and ethanol ( $C_2H_5OH$  99.5%) (obtained by CTR, Nuevo León México).

Basic blue 9 reagent (obtained by EMD chemicals, Gibbstown, NJ) was used to prepare the methylene blue ( $C_{16}H_{18}N_3SCl \cdot 3H_2O$ ) (CAS 61-73-4) solutions.

## 2.2. Deposition of CdS thin films

The CdS films were deposited by immersion of the glass substrates in a CBD solution according to [40-41] prepared from cadmium chloride ( $\text{CdCl}_2$ ), sodium citrate ( $\text{Na}_3\text{C}_6\text{H}_5\text{O}_7$ ), pH 10 borates buffer, potassium hydroxide (KOH), and thiourea ( $\text{SC}(\text{NH}_2)_2$ ) in a volumetric ratio of 9 ml (0.05M): 9 ml (0.5 M): 3 ml: 3 ml (0.5 M): 4.5 ml (0.5M). The total reaction volume was adjusted with water to 60 ml. In [40-41] CdS thin films deposited by CBD on  $\text{HfO}_2$  is reported at  $70^\circ\text{C} \pm 1^\circ\text{C}$  for 25 minutes, in this work to achieve thin films deposition on glass substrate we adjusted the temperature of the solution at  $43^\circ\text{C} \pm 1^\circ\text{C}$  for 33 minutes, also here the chemical deposition process was repeated two consecutive times with fresh solutions used for every deposition in order to obtain homogeneous and structural representative CdS material, considering that the temperature from original recipe was reduced and the deposition time was increased.

After deposition, the CdS films were cleaned firstly, exposed in an ultrasonic bath with methanol followed by distilled water rinse and dried with  $\text{N}_2$ .

## 2.3. Preparation of $\text{TiO}_2$ nanoparticles (Nps)

The synthesis of the  $\text{TiO}_2$  Nps, is realized by a microwave assisted sol gel process according to [42], where the precursor solution consist into dissolve titanium isopropoxide in 2-propanol at a volume ratio of 1: 15 (2.72 ml: 40 ml), then are stirred vigorously for 700 rpm during 1 min at  $80^\circ\text{C}$ , in order to enhance the homogeneity and stability of the slurry, after that a volume ratio of 1:2 (0.52 ml: 1 ml) a mix of deionized water and 2-propanol was added, the final solution was kept in stirring during 2 min at  $80^\circ\text{C}$ .

The sol formed was allowed to age under room temperature conditions for 24 hrs. After 24 hours, a transparent solution (supernatant) was extracted and the precipitate was exposed to microwaves for drying, remaining a total time of 15 minutes. After this process, the  $\text{TiO}_2$  nanoparticles were obtained as the settled powder in the container. This drying assisted by microwaves enabled uniform heating of the forming  $\text{TiO}_2$  nanoparticles, maintaining their shape and reducing the production of sub-products and the risk of structural damage (1). Finally, the powder of the  $\text{TiO}_2$  nanoparticles was carefully washed with deionized water to remove any matter other than  $\text{TiO}_2$ .

### 2.3.1. $\text{TiO}_2$ Nps thin film

The  $\text{TiO}_2$  Nps obtained were dispersed in ethanol and deposited on glass substrate at room temperature by spin coating technique. The spinning speed was established at 1000 rpm for 30 s at room temperature.

## 2.4. $\text{TiO}_2$ NPs/CdS thin films/Glass substrate, preparation

The  $\text{TiO}_2$  Nps films were deposited on CdS thin films. The CdS deposited on glass substrate was placed in the spin coater (anticorrosion 6" wafer Max) and was completely covered with 1 ml of the  $\text{TiO}_2$  Nps dispersed in ethanol (0.004 gr of  $\text{TiO}_2$  Nps/ 1ml ethanol). The spinning speed was established at 1000 rpm for 30 s at room temperature. The drying step was performed by heating thin film at a temperature of  $75^\circ\text{C}$  for 15 min in a Labnet accuplate hotplate in air atmosphere.

## 2.5. Materials Characterization

Optical absorption measurements were performed using a Jeneway 6850 UV/visible spectrophotometer in the range from 300 to 900 nm. The morphology and elemental compositions for films and nanoparticle size were characterized by Scanning Electron Microscopy (SEM) on a Hitachi SU5000 with operating voltage of 20 kV. The crystalline structures of the CdS thin films and the  $\text{TiO}_2$  nanoparticles were examined by X-ray diffraction (XRD) using a PANalytical, US. The diffractometer is equipped with a  $\text{CuK}$  source, operating at 35 kV and 23 mA, the scans were taken in a  $2\theta$  range from 10 to  $80^\circ$ .

## 2.6. Photocatalytic degradation of methylene blue (MB)

The photocatalytic activity of TiO<sub>2</sub> NPs/ CdS thin films was evaluated through the degradation of the organic dye MB as a model for organic pollutant [31], in the presence of the radiation of the sun for 60 minutes. Experimental data conditions for three replicates for photocatalysis, is shown in Table 1.

To prepare the aqueous solution, 50 ml of MB were introduced into a beaker at a concentration of 20 mg/L and kept under stirring at 1000 rpm. To initiate photocatalytic study, TiO<sub>2</sub> NPs/CdS thin films/Glass substrate, were introduced to allow their interaction with the solution for 60 minutes under sunlight.

The MB concentration was determined by measuring the intensity of absorption through a UV-Vis spectrophotometer in a wavelength range of 300-900 nm.

Table 1. Conditions of photocatalytic reaction (Ciudad Juárez, Chihuahua, México).

Conditions/Number of replicas	1	2	3
Date of reaction	November 13, 2018 (12:40 to 13:40)	March 29, 2019 (13:15 to 14:15)	August 26, 2019 (14:00 to 15:00)
Solar radiation (W/m <sup>2</sup> )	562.20	870.72	825.63
solar UV index	2.57	6.60	7.13
C <sub>0</sub> (mg/L)	20.332	20.165	20.263

In order to quantify the degradation of the dye, a calibration curve was first made on a PerkinElmer Lambda 25 UV-Vis spectrometer at known concentrations of 5, 10, 15 and 20 mg/L.

## 3. Results and discussions

### 3.1. Characterization of CdS thin films

#### 3.1.1. Optical characterization of CdS thin films

The UV-Vis spectra of CdS films prepared by chemical bath deposition is shown in Figure 1a. The spectra exhibit a well-defined feature (peak) at ~527 nm, which is considerably blue-shifted relative to the peak absorption of bulk CdS indicating quantum size effect [28-43].

The UV-Vis transmission spectra of the CdS films shown that the material can be excited with the visible light corresponding to the values between 450 and 750 nm [44] (Figure 1a). The optical band gap was calculated from the data obtained using the equation 1 below (Tauc plot method) [45], resulting in the value of 2.89 eV (Fig. 1b).

$$(\alpha h\nu) = A(h\nu - E_g)^n \quad (1)$$

In equation 1,  $\alpha$ ,  $h\nu$ ,  $A$ , and  $E_g$  correspond to the absorption coefficient, the incident photon energy (Planck constant and light vibration frequency), proportionality constant, and band gap energy. Finally,  $n$  is a constant having value  $\frac{1}{2}$  for direct band gap and 2 for indirect band gap, respectively [46].

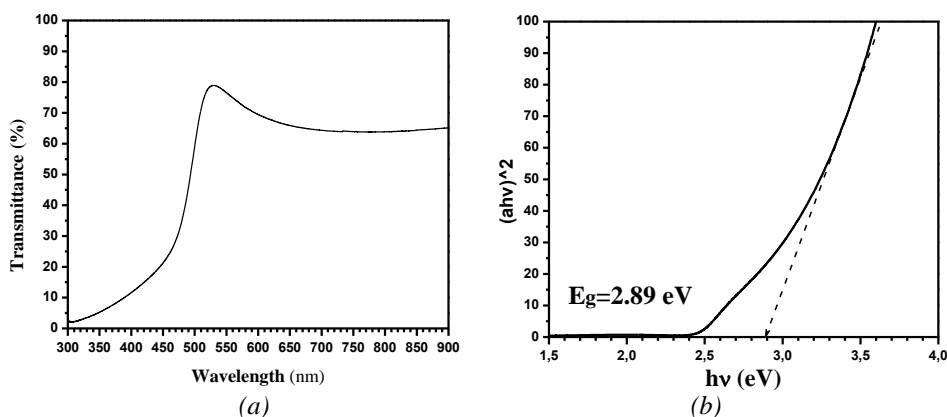


Fig. 1. (a) UV-Vis transmission spectra obtained for a CdS thin film deposited by CBD; (b) Tauc variable vs Energy.

### 3.1.2. CdS thin films morphology

Fig. 2a shows homogeneous morphology at the surface for CdS thin films deposited. Average CdS thicknesses was obtained by SEM cross-section (Fig. 2b). The resulting thicknesses value is 169 nm.

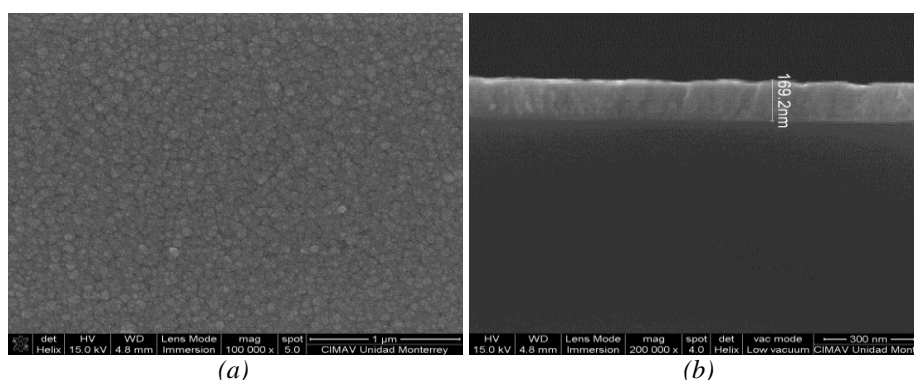


Fig. 2. SEM micrographs for CdS thin films deposited by CBD a) surface and b) cross-section.

### 3.1.3. X-ray diffraction (XRD)

Fig. 3 shows the XRD patterns obtained for the CdS thin film deposited by CBD. The X-ray diffraction peak located at  $2\theta = 26.6^\circ$  shows the preferential orientation along the (002) hexagonal plane. Carrillo *et al.* previously reported the same phase in CdS thin films [23].

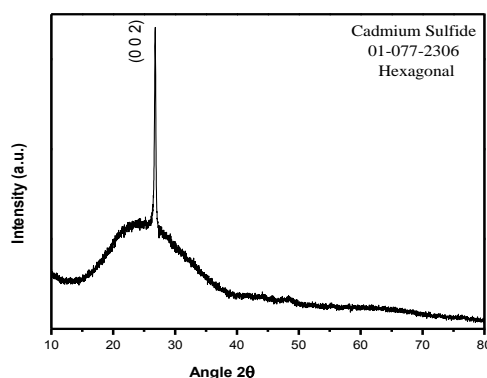


Fig. 3. XRD pattern for CdS thin films by CBD.

### 3.2. Characterization of TiO<sub>2</sub> nanoparticles (Nps)

#### 3.2.1. Optical characterization of the TiO<sub>2</sub> NPs

Fig. 4a shows the UV-Vis transmission spectra of TiO<sub>2</sub> Nps thin film. The spectra show that the nanoparticles stop transmitting light in the UV region, which means absorption is occurring in this spectral region. This also indicates that the nanoparticles are activated (excited) in that region, where the activation is understood as the occurrence of the electrons jump from the valence band to the conduction band, leaving a hole with positive charge in the valence band [47]. Fig. 4b shows the TiO<sub>2</sub> band gap energy of 3.9 eV, indicating that the photons that impinge on the material with a wavelength in the UV region do not need as much energy to excite the TiO<sub>2</sub> nanoparticles.

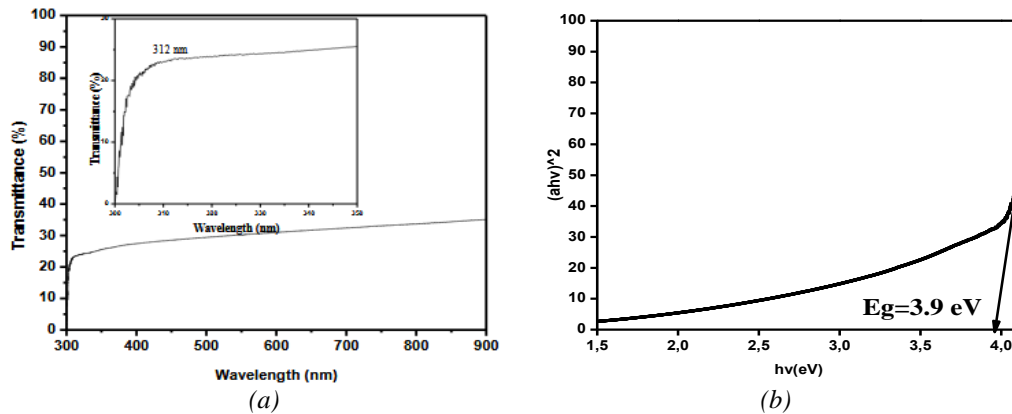


Fig. 4. (a) UV-Vis transmission spectra obtained for TiO<sub>2</sub> Nps thin film and (b) Tauc variable vs Energy.

#### 3.2.2. TiO<sub>2</sub> NPs morphology characterization

The micrograph in Fig. 5a) shows agglomerated TiO<sub>2</sub> nanoparticles at a magnification of 18KX, which were deposited in a mesh for observation. Fig. 5b shows the approximate sizes of nanoparticles, which have diameters from 3.16 to 5.39 nm. Agglomerated nanoparticles were also observed by [28].

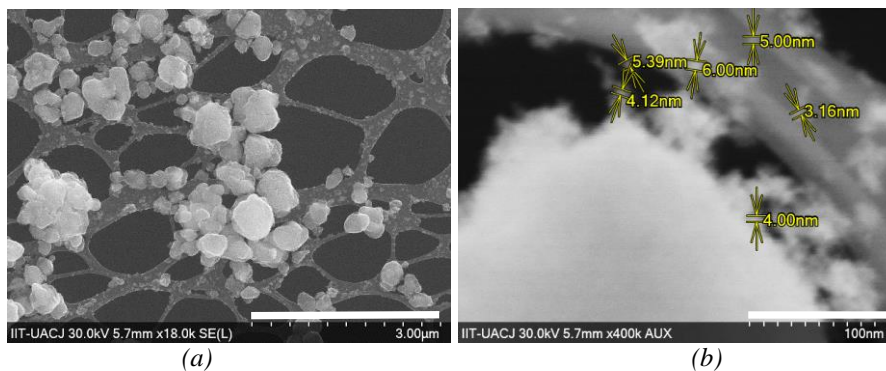


Fig. 5. SEM micrographs for TiO<sub>2</sub> nanoparticles.

#### 3.2.3. X-ray diffraction (XRD) of the TiO<sub>2</sub> nanoparticles

Fig. 6 shows the XRD pattern for TiO<sub>2</sub> nanoparticles, where the main diffraction peaks occur at 2θ angles of 25°, 28°, 31°, 36°, 38°, 48°, 54° and 64°. The peaks at 12° and 31° are not of these TiO<sub>2</sub> crystallographic phases.

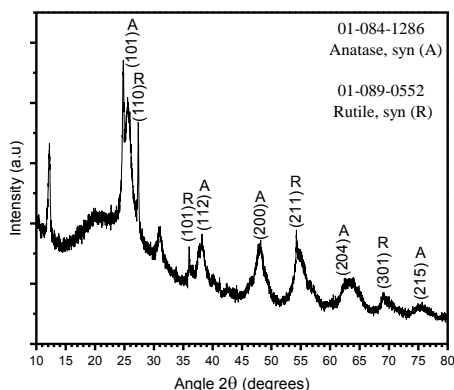


Fig. 6. XRD pattern for  $\text{TiO}_2$  NPs. The planes corresponding to their corresponding reference code.

The indexation of these peaks corresponds to the crystalline structure of the rutile and anatase phases of  $\text{TiO}_2$ , indicating the polymorphism of this material. The indexed peaks at (101), (200) and (204), correspond to anatase phase having a tetragonal crystal structure, while the peaks (110) and (211) are attributed to the signals of the rutile phase with hexagonal crystal structure [48].

### 3.3. Characterization of the $\text{TiO}_2$ NPs/CdS thin films

#### 3.3.1. Optical characterization of the $\text{TiO}_2$ NPs/CdS thin films

Transmission spectra of the system deposited of  $\text{TiO}_2$ /CdS films are shown in Fig. 7, it can be seen that the film show bands at 349-530. According to the spectra on Fig. 1 and 4 for CdS and  $\text{TiO}_2$  thin films respectively red shift is observed when the materials are coupled, where  $\text{TiO}_2$  NPs/CdS thin films presented absorption on UV and visible region (between 300 and 600 nm) and the electrons of the material are exciting with less energy from photons. This noticeable shifting and the intensity changes on the bands are ascribed to the bonding and the interaction between  $\text{TiO}_2$  and the CdS. The determinate band gap energy of the thin film of  $\text{TiO}_2$ /CdS is 2.8 eV (Fig. 7b).

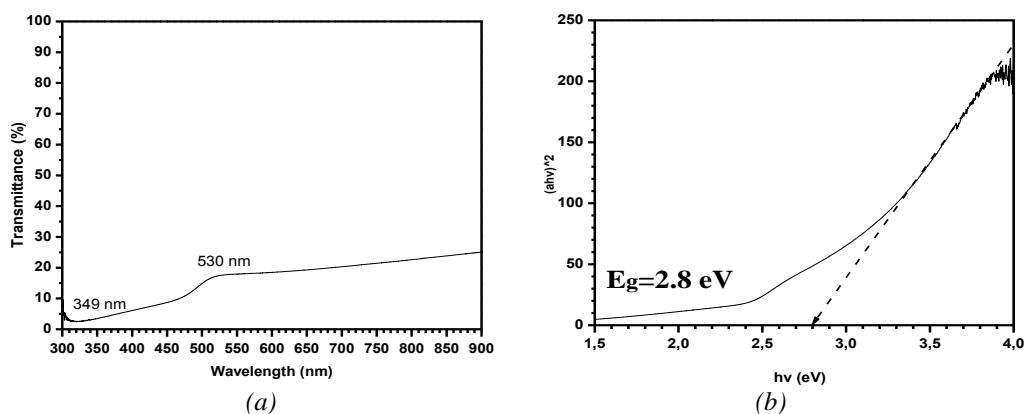


Fig. 7. a) UV-Vis transmission spectra for a  $\text{TiO}_2$  NPs/CdS thin film, b) Tauc variable vs Energy.

#### 3.3.2. Morphology characterization of $\text{TiO}_2$ NPs/CdS thin films

Fig. 8a and 8b shows a homogeneous surface of CdS (the CdS appearing as the darker gray color), with agglomerated  $\text{TiO}_2$  nanoparticles covering it (the agglomerated nanoparticles are color white).

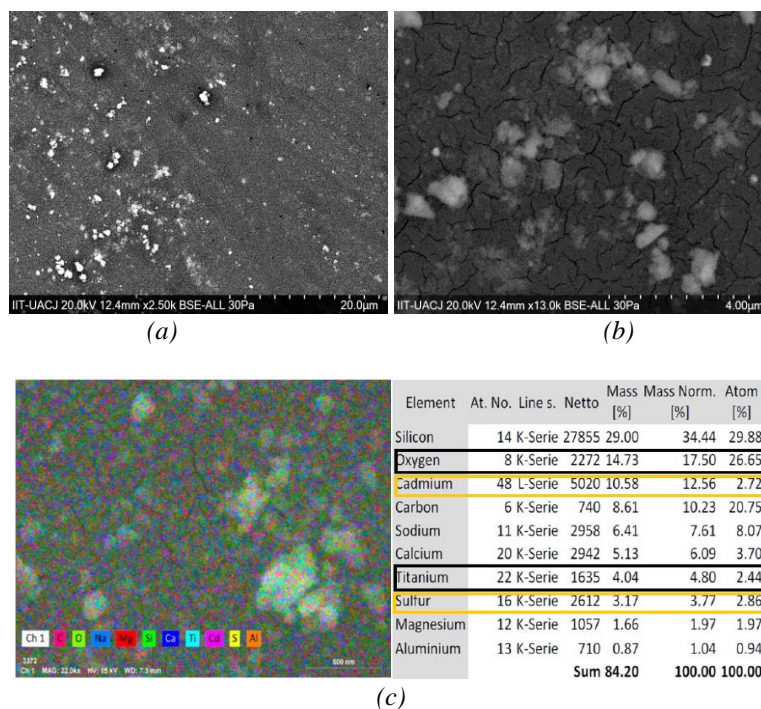


Fig. 8. (a) and (b) SEM micrographs and (c) EDAX analysis for  $\text{TiO}_2/\text{CdS}$  thin films.

The images indicate that no full coverage of the  $\text{TiO}_2$  on the CdS film is achieved. Fig. 8b shows more detail of this effect and no full coverage was achieved where no complete homogeneity of the nanoparticles is seen. This non homogeneous dispersion of  $\text{TiO}_2$  nanoparticles on CdS can be attended with future work where the dispersion of the nanoparticles can be improved for their subsequent deposit in thin film, however this did not influence to achieve a photocatalytic activity of the proposed system of  $\text{TiO}_2$  NPs /CdS thin films, as is explained in the next section. Also, it is observed by means of EDAX (Fig. 8c) that the elemental distribution of Cd, S, Ti and O is homogeneous with atomic percentages relation according of chemical composition for CdS and  $\text{TiO}_2$ .

### 3.4. Photocatalytic test

#### 3.4.1. Optical characterization of methylene blue

The UV-visible spectrum of MB solution (20.253 mg/L) displays an absorbance at two bands with maxima 663 nm and a hump at around 610 nm corresponding to the absorption bands of the monomeric and dimeric species respectively as reported (Fig. 9 black dotted line) [49].

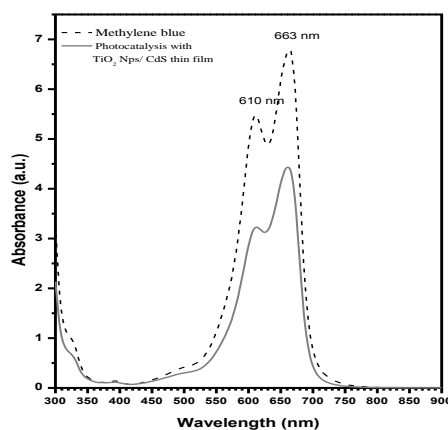


Fig. 9. Absorption spectrum of a solution of methylene blue concentration before and after of 60 minutes of heterogeneous photocatalysis.

Fig. 9 also shows that the absorbance intensity of MB after heterogeneous photocatalysis with TiO<sub>2</sub> Nps films/CdS thin films, versus the wavelength decreases dramatically and no new bands appear, which indicates that the MB (monomer and dimer) can be decomposed. It can be acknowledged that the discoloration occurs at the same time, and MB can be decomposing, where the photocatalytic reactions promote the oxidative capacity in the system causes the acceleration of photoreaction as can be seen in Fig. 9, causing a decrease in the MB concentration of 43%, thus checking the ability of the films CdS and TiO<sub>2</sub> Nps to recombine electron pairs hollow generating hydroxyl radicals •OH when they interact with MB.

The photocatalytic tests can take up to 5 hours to obtain a high photodegradation performance [50].

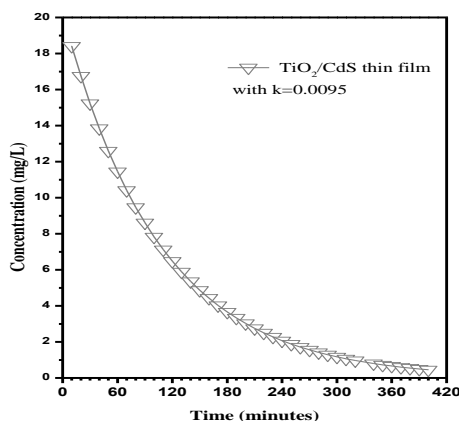


Fig. 10. Reaction kinetics of methylene blue degradation.

In this work, a reaction time of 60 minutes was employed to obtain the initial variables and the reaction constant (k). In this calculation, the following differential equation (equation 2) of first order used:

$$\frac{dC}{dt} = -kC \quad (2)$$

Solving this equation gives equation 3:

$$C(t) = C_0 e^{-kt} \quad (3)$$

Solving equation 3 for k yielded:

$$k = -\frac{\ln\left(\frac{C_t}{C_0}\right)}{t} \quad (4)$$

Finally, equation 4 was solved using the values obtained experimentally for C<sub>0</sub> (20.253 mg/L), C(t) 11.4934mg/L and t: 60 minutes. Accordingly, thus the kinetics of MB degradation are shown in Figure 10, which indicates that the dye degrades 50% after 100 minutes considering that it can vary due to the weather conditions found at the time of the heterogeneous solar photocatalysis.

Fig. 11 indicate the concentration of the replicates as well as the standard deviation of the replicates, the experimentation has standard deviation due solar radiation is different every day.

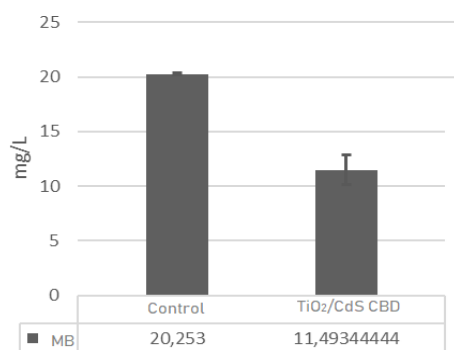


Fig. 11. Error bars indicate standard deviations and concentrations of triplicate experiments.

#### 4. Conclusions

This work has reported, for the first time, on the successful synthesis of a new material obtained by soft chemistry at low temperature composed for TiO<sub>2</sub> NPs/CdS thin film/Glass substrate used in heterogeneous photocatalysis to degrade an organic compound as Methylene Blue. The photocatalytic activity presented 42-43 % of MB degradation within 60 minutes. This new material and photocatalytic process can be extended to apply in the treatment of industrial wastewater containing others organic pollutants.

#### Acknowledgements

The authors acknowledge partial financial support from CONACyT through the grants Becas Nacionales (CVU: 500846), ByNEF group as well as personnel from UABC is acknowledge. They also wish to thank Ph.D., Marcela Mireles, Ph.D., Cesar Terrazas and Ph.D. Natalia Noriega for technical support.

#### References

- [1] Y. Wang, Y. He, Q. Lai, M. Fan, JES **26**(11), 2139 (2014).
- [2] D. Štrbac, C. A. Aggelopoulos, G. Štrbac, M. Dimitropoulos, M. Novaković, T. Ivetić et al., Process Saf Environ Prot. **113**, 174 (2018).
- [3] R. Molinari, C. Lavorato, P. Argurio, Catal Today **281**, 144 (2017).
- [4] M. E. Borges, M. Sierra, J. Méndez-Ramos, P. Acosta-Mora, J. C. Ruiz-Morales, P. Esparza, Sol Energy Mater Sol Cells **155**, 194 (2016).
- [5] L. Zhong, F. Haghghat, Build Environ **91**, 191 (2015).
- [6] R. Fiorenza, A. Di Mauro, M. Cantarella, A. Gulino, L. Spitaleri, V. Privitera et al., Mater Sci Semicond Process **112**, 105019 (2020).
- [7] F. V. S. Lopes, R. A. R. Monteiro, A. M. T. Silva, G. V. Silva, J. L. Faria, A. M. Mendes et al., Chem. Eng. J. **244**, 204 (2012).
- [8] E. Zghab, M. Hamandi, F. Dappozze, H. Kochkar, M. S. Zina, C. Guillard et al., Mater. Sci. Semicond. Process **107**, 104847 (2019).
- [9] C. Dong, J. Liu, M. Xing, J. Zhang, Res. Chem. Intermed. **44**(11), 7079 (2018).
- [10] Q. Zhou, Z. Fang, J. Li, M. Wang, Microporous Mesoporous Mater **202**(C), 22 (2015).
- [11] Y. Wang, Y. He, Q. Lai, M. Fan, J. Environ. Sci. **26**(11), 2139 (2014).
- [12] N. Yao, K. Lun Yeung, Chem Eng J. **167**(1), 13 (2011).
- [13] N. Yao, K. Lun Yeung, Chem. Eng. J. **167**(1), 13 (2011).
- [14] Y. Hu, X. Song, S. Jiang, C. We, Chem. Eng. J. **274**(x), 102 (2015).
- [15] Rashad AESMRMM, Organic acid precursor synthesis and environmental photocatalysis Applications of mesoporous anatase TiO<sub>2</sub> doped with different transition metal ions, 3141 (2014).

- 
- [16] Z. Shi, J. Liu, H. Lan, X. Li, B. Zhu, J. Yang, *J. Mater. Sci. Mater. Electron* **30**(19), 17682 (2019).
- [17] B. Zeng, W. Liu, W. Zeng, C. Jin, *Chalcogenide Lett.* **10**(2), 73 (2019).
- [18] N. Balpınar, F. Gode, *Chalcogenide Lett.* **17**(9), 429 (2020).
- [19] H. L. Meng, C. Cui, H. L. Shen, D. Y. Liang, Y. Z. Xue, P. G. Li et al., *Synthesis and photocatalytic activity of TiO<sub>2</sub> @ CdS and CdS @ TiO<sub>2</sub> double-shelled hollow spheres* **527**, 30 (2012).
- [20] Q. Shen, J. Xue, H. Zhao, M. Shao, X. Liu, H. Jia, *J. Alloys Compd.* **695**, 1080 (2017).
- [21] A. Carrillo-Castillo, R. C. Ambrosio Lázaro, E. M. Lira Ojeda, C. A. Martínez Pérez, M. A. Quevedo-López, F. S. Aguirre-Tostado, *Chalcogenide Lett.* **10**(10), 421 (2013).
- [22] A. Ahmad Beigi, S. Fatemi, Z. Salehi, *J. CO<sub>2</sub> Util* **7**, 23 (2014).
- [23] P. Zhou, Y. Xie, J. Fang, Y. Ling, C. Yu, X. Liu et al., *Chemosphere* **178**, 1 (2017).
- [24] S. Peng, Y. Huang, Y. Li, *Mater. Sci. Semicond. Process* **16**(1), 62 (2013).
- [25] P. Zhou, Y. Xie, J. Fang, Y. Ling, C. Yu, X. Liu et al., *Chemosphere* **178**, 1 (2017).
- [26] S. Peng, Y. Huang, Y. Li, *Mater. Sci. Semicond. Process* **16**(1), 62 (2013).
- [27] Na Qin, Yuhao Liu, Weiming Wu, Lijuan Shen, Xun Chen, Zhaohui Li, Ling Wu, *Langmuir* **31**, 1203 (2015).
- [28] Jian-Wen Shia, Xiaoxia Yan, Hao-Jie Cui, Xu Zong, Ming-Lai Fu, Shaohua Chen, Lianzhou Wang, *Journal of Molecular Catalysis A: Chemical* **356**, 53 (2012).
- [29] A. Kaura, A. William, A. Sushil, K. Kansala, *Photochemistry and Photobiology A: Chemistry* **360**(1), 34 (2018).
- [30] L. Liu, H. Hou, L. Wang, R. Xu, Y. Lei, S. Shen, W. A. Yang, *Nanoscale* **9**(40), 15650 (2017).
- [31] A. Hamdi, D. P. Ferreira, A. M. Ferraria, D. S. Conceição, L. F. Carapeto, S. Boufi, S. Bouattour, A. M. Botelho do Rego, *Journal of Nanomaterials* **2016**, Article ID 6581691, 11 pages.
- [32] Sessa S. Srinivasan, Jeremy Wade, Elias K. Stefanakos, *Journal of Nanomaterials* **2006**, Article ID 87326.
- [33] P. Nyamukamba, M. Moloto, H. Mungondori, *Journal of Nanotechnology*, **2019**, Article ID 5135618, 10 pages.
- [34] S. Qian, C. Wang, W. Liu, Y. Zhu, W. Yao, X. Lu, *J. Chem.* **21**, 4945 (2011).
- [35] X. Cheng, Y. Shang, Y. Cui, R. Shi, Y. Zhu, P. Yang, *Solid State Sciences* **99**, 106075 (2020).
- [36] G. Liu, W. Jia, Q. Jiangb, Z. Cheng, *Controllable growth of three-dimensional CdS nanoparticles on TiO<sub>2</sub> nanotubes to enhance photocatalytic activity.*
- [37] B. Krishnan, R. Menon, *J. Nanosci. Tech.* **5**(4), 791 (2019).
- [38] J. Song, D. Zeng, Y. Xie, F. Zhang, S. Rao, F. WanG, J. Zhao, J. Zhang, L. Wang, *Preparation of CdS Nanoparticles-TiO<sub>2</sub> Nanorod Heterojunction and Their High-Performance Photocatalytic Activity, Catalyst.*
- [39] D. Spasiano, R. Marotta, S. Malato, P. Fernandez-Ibañez, I. Di Somma, *Appl. Catal. B Environ.* **90**, 170 (2015).
- [40] A. L. Sallas Villasenor, I. Mejia, J. Hovarth, H. N. Alshareef, D. K. Cha, R. Ramirez Bon, B. E. Gnade, M. A. Quevedo Lopez, *Electrochem. Solid State Lett.* **13**(9), H313 (2010).
- [41] A. Carrillo, F. Aguirre, A. Salas, I. Mejía, B. E. Gnade, M. Sotelo, M. Quevedo, *Chalcogenide Letters* **10**(2), 81 (2013).
- [42] M. Mota-González, H. Hernández-Carrillo, M. Alaniz-Hernandez, F. Morales-Olazoc, A. Carrillo-Castillo, *Latin American Journal of Applied Engineering* **3**(1), 1 (2018).
- [43] K. S. Suslick, *J. Acoust. Soc. Am.* **89**(4B), 1885 (1991).
- [44] M. Antoniadou, V. M. Daskalaki, N. Balis, D. I. Kondarides, C. Kordulis, P. Lianos, *Applied Catal. B Environ.* **107**(1–2), 188 (2011).
- [45] A. K. Vishwakarma, P. Tripathi, A. Srivastava, A. S. K. Sinha, O. N. Srivastava, *Int. J. Hydrogen Energy* **42**(36), 22677 (2017).
- [46] M. Wang, H. Zhang, H. Zu, Z. Zhang, J. Han, *Appl. Surf. Sci.* 2018.
- [47] J. Tao, Z. Gong, G. Yao, Y. Cheng, M. Zhang, J. Lv et al., *Ceram. Int.* **42**(10), 11716 (2016).

---

[48] M. Tahir, N. S. Amin, *Applied Catal. A Gen.* **467**, 483 (2013).

[49] T. Sagara, K. Niki, *Langmuir* **9**(3), 831 (1993).

[50] W. Vallejo, C. Diaz-Urbe, A. Cantillo, *J. Photochem. Photobiol. A Chem.* **299**, 80 (2015).